Yonago Acta medica 2005;48:63–74

Cell Death Induction of Thymidine Kinase Gene Transfer Followed by Ganciclovir Treatment in Oral Squamous Cell Carcinoma Cell Lines

Itaru Kuratate*†, Mitsuhiko Osaki* and Kazuo Ryoke†

**Division of Organ Pathology, Department of Microbiology and Pathology, †Division of Oral and Maxillofacial Biopathological Surgery, Department of Medicine of Sensory and Motor Organs, School of Medicine, Tottori University Faculty of Medicine, Yonago 683-8503 Japan*

The tumoricidal effect of herpes simplex virus thymidine kinase (HSV-tk) gene transfer followed by ganciclovir (GCV) treatment has been demonstrated in relation to the bystander effect. We examined the mode of cell death after GCV treatment in three human oral squamous cell carcinoma (SCC) cell lines that had been infected with adenovirus possessing HSV-tk gene. Oral SCC cell lines displayed high susceptibility to HSV-tk/GCV treatment despite low transduction. Evidence suggests that apoptosis was not found by internucleosomal DNA fragmentation, cell cycle kinetics or gene expressions indicative of apoptosis. However, we observed different levels of expression of annexin V-positive/propidium iodide-negative cells in all the cell lines and occasional TUNEL-positive cells in one cell line. To address these controversial findings, we further confirmed the morphological phenotypes of cell death with semi-thin and ultra-thin sections, which revealed that the cells undergoing death were consistent with necrosis, i.e. swelling of cytoplasm and intracellular organs with membrane disruption. Furthermore, no apoptotic bodies were detected within cytoplasm of apparently intact cells. A nonapoptotic mechanism may play a central role in the HSV-tk/GCV-induced cell death in oral SCC cell lines.

Key words: apoptosis; ganciclovir; necrosis; thymidine kinase

Squamous cell carcinoma (SCC) is the most frequent malignancy in the oral cavity. The prognosis of advanced oral SCC has remained poor over the last few decades despite progress in aggressive approaches using combination therapy. Novel strategies should be explored in the oral cancer field.

One of the potential improvements in current therapeutic strategies is herpes simplex virus thymidine kinase (HSV-tk) gene transfer followed by ganciclovir (GCV) treatment based on the enzyme/prodrug system concept (Borrelli et al., 1988). HSV-tk-transduced cells selectively convert prodrug GCV into monophosphate GCV. Triphosphate GCV is the final activated form with an ability to kill cells by interfering in DNA synthesis through chain termination and single-strand breaks (Elion, 1982). Another promising aspect of this strategy is the existence of the so-called "bystander effect" (Freeman et al., 1993; Colombo et al., 1995), which mediates cytotoxicity to the adja-

Abbreviations: Ad, adenovirus; FITC, fluorescein isothiocyanate; GCV, ganciclovir; HSV-tk, herpes simplex virus thymidine kinase; IC50, median inhibitory concentration; MOI, multiplicity of infection; PBS, phosphate-buffered saline; pfu, plaque forming unit; PI, propidium iodide; SCC, squamous cell carcinoma; TUNEL, terminal deoxynucleotidyl transferase-mediated dUTP-digoxigenin nick-end labeling

Table 1. Oral squamous cell carcinoma cell lines and *p53* status

Cell line	Histology*	*p53* status	Mutation	Site mutation codon
HSC-3	por	mutant	exon8	TAAG insersion (305 and 306)
HSC-4	well	mutant	exon7	248CGC to CAG
SCCKN	mod	mutant	exon5	178CAC to -AC (frame shift)

*well, well differentiated type; mod, moderately differentiated type; por, poorly differentiated type.

cent untransduced cells. There have been two hypothesis proposed to explain the bystander effect: (i) transfer of cytotoxic molecules via gap junctions because phosphorylated GCV is unable to diffuse freely across the cytoplasmic membrane (Bi et al., 1993) and (ii) phagocytosis of apoptotic bodies containing GCV-metabolites from HSV-tk-transduced cells by untransduced intact cells (Freeman et al., 1993; Colombo et al., 1995).

HSV-tk/GCV treatment has been successfully applied in both human and animal tumor cell lines of different origins (Moolten et al., 1990; Glaser et al., 2001; Lanuti et al., 1999; Li et al., 1999; Boucher et al., 1998). There have been, however, few studies on oral SCC cell lines (O'Malley et al., 1996; Fukui et al., 2001). While the validity of this approach has been confirmed, the molecular mechanism of HSV-tk/GCV-induced cell death remains to be elucidated. The most commonly described cell death mechanism was related to the induction of apoptosis, not only for the execution pathway but also the bystander effect (Colombo et al., 1995; Samejima and Maruelo, 1995). On the other hand, a few studies have suggested nonapoptotic induction, i.e. necrosis (Kaneko and Tsukamoto, 1995; Vile et al., 1997; Katabi et al., 2002). Recently, activation of caspase-independent apoptotic pathways was also suggested because of the incomplete inhibition of cell death by caspase inhibitors such as z-VAD-fmk (Beltinger et al., 1999; Rivas et al., 2001). Both molecular biological analysis and morphological examinations are indispensable for apoptotic evaluation. Most studies exposing the HSV-tk/GCV-induced cell death mechanism have been performed with apoptosis-related molecular biological analysis, while a few studies using ultrathin examinations have been performed where apoptosis was originally evaluated from the morphological changes that occurred at ultra-structural levels (Kerr et al., 1972).

The purpose of the present study was to assess the feasibility of adenovirus-mediated HSV-tk gene transfer followed by GCV to oral SCC cell lines, in addition to verifying whether apoptotic responses are associated with HSV-tk/GCV-induced cell death. In addition, we examined the ultrastructural level alterations to identify molecular biological changes.

Materials and Methods

Cell lines

Three cell lines derived from human tongue SCCs were used (Table 1). We obtained HSC-3 and HSC-4 from the Health Science Research Resources Bank (Osaka, Japan), and SCCKN from Riken Gene Bank (Tsukuba, Japan). Cell line 293 derived from human embryonic kidney was used for both virus purification and titer determination. All cell lines were grown in Dulbecco's MEM (COSMO BIO, Tokyo, Japan) complemented with 1/100 diluted Gibco solution (29.2 mg/mL L-glutamine 10,000 unit/mL penicillin G, 10,000 μg/mL streptomycin) and 10% inactivated fetal bovine serum and maintained at 37˚C in an incubator under 5% CO_2/95% air atmosphere.

Adenovirus vectors

Two replication-deficient recombinant adenoviruses containing LacZ marker gene (Ad.β-gal) as a control and luciferase vector, and adenoviruses containing HSV-tk (Ad.tk) as the therapeutic vector under the control of cytomegalovirus promoter

were kindly provided from Professor Kenzo Sato (Division of Molecular Biology, Department of Molecular and Cellular Biology, School of Medicine, Tottori University Faculty of Medicine, Yonago, Japan). The Ad.β-gal and Ad.tk were propagated in 293 cells, which include the Ad5 E1 region in chromosomal DNA. These viruses were purified by sequential centrifugation in CsCl step gradients. Virus titers were determined as plaque forming units (pfu) using a modified end-point cytopathic effect assay. The titers of stock in 5% glycerol and 95% culture medium of Ad.β-gal and Ad.tk were 2.27×10^{10} pfu/mL and 1.35×10^{11} pfu/mL, respectively.

Adenovirus infection efficiency

Cells were seeded in 24-well culture plates at a density of 2×10^4/well. After overnight incubation, stock Ad.β-gal was diluted in 100 μL of medium and added at varying multiplicities of infection (MOIs) of 0, 6.25, 12.5, 25, 50 or 100. The cells were exposed for 1 h with constant agitation, and then the fresh medium was added up to 500 μL. Plates were incubated for an additional 24, 48 and 72 h at 37˚C. After rinsing with phosphate-buffered saline (PBS) twice, cells were fixed with a solution of 2% formaldehyde and 0.2% glutaraldehyde in PBS for 10 min at 4˚C. Cells were rinsed with PBS twice and incubated in a solution containing the X-gal (0.2% 5-bromo-4-chloro-3-indolyl-β-D-galactopyranoside) for 4 h at 37˚C. The number of blue cells expressing transgene was counted. Adenovirus infection efficiency was expressed as a mean of the percentage of stained cells to the total cells from three randomly selected microscopic fields at ×200 magnification.

Cell viability assay

Cells were seeded in 60 mm dishes at a density of 3×10^5/dish. After overnight incubation, both stock Ad.β-gal and Ad.tk were diluted in 100 μL of medium and adjusted at MOIs of 1.25, 5, 10 and 20. Each dish was exposed for 1 h with viral diluted medium or condition medium, and then fresh medium was added up to 300 μL. After 16 h incubation at 37˚C, cells were trypsinized and replated in 96-well culture plates at a density of 3×10^3/well. After overnight incubation, the medium was replaced with selective 100 μL medium containing different concentrations of GCV (0–1,000 μg/mL). Uninfected cells without GCV treatment were also incubated as controls. Cell viability was assessed at 96 h after GCV treatment using an MTT assay (CellTiter 96 Nonradioactive Cell Proliferation Assay, Promega, Madison, WI). According to the manufacturer's instruction, 15 μL of the dye solution was added to each well and the plates were incubated for 4 h. Subsequently, 100 μL of the solubilizing solution was added. After overnight incubation, the absorbance at 570 nm wavelength was measured using a microplate reader. Cell viability was expressed as the relative percentage to control. The result represents the mean ± SE of triplicates.

DNA fragmentation

Both floating and attached cells were harvested from wells at 0, 12, 24, 48 and 72 h incubation times after HSV-tk/GCV treatment. Cells were incubated for 10 min at 4˚C in 100 μL lysis buffer containing 10 mM Tris-HCl (pH 7.4), 10 mM EDTA and 0.5% Triton X-100. After centrifugation for 5 min at 16,000 rpm, the supernatants were decanted and digested with RNase A (100 μg/mL, final) at 37˚C for 1 h and then with proteinase K (200 μg/mL, final) for 1 h at 37˚C. After these treatments, DNA was extracted by phenol, and isopropanol precipitation. These preparations were subjected to electrophoresis in 2% agarose gels and stained with 0.5 μg/mL ethidium bromide and electrophoretic patterns of the gel under UV light was photographed.

Cell cycle kinetics

Cells were infected with Ad.tk at MOIs of 5 for HSC-3 or 2.5 for HSC-4 and SCCKN, respectively. After 16 h incubation, the medium was exchanged with GCV medium at a concentration of 1 μg/mL. Both floating and attached cells were harvested from wells at 0, 12, 24, 48 and 72 h incubation times after HSV-tk/GCV treatment. Then, 1×10^6/mL

suspensions were prepared for flow cytometry assay.

To analyze cell cycle kinetics, 2×10^5 cells were fixed in 70% ethanol and stored at 4˚C until ready for use. Cells were centrifuged and resuspended in 1 mL PBS containing RNaseA (DNase free, 0.1 mg/mL), and stained with 50 μg/mL propidium iodide (PI). Samples were analyzed within 1 h after the staining procedure. Fluorescence intensity was determined by an EPICS XL flow cytometer (Coulter, FL).

Annexin V assay

To detect the early stage of apoptosis, annexin V-fluorescine isothiocyanate (FITC) and PI double staining were performed according to the manufacturer's instructions for the apoptosis detection kit (Trevigen, MD). Briefly, 1×10^5 cells were exposed with 100 μL of labeling reagent containinig 1 μL of annexin V-FITC conjugate and 10 μL of PI (50 μg/mL). After 15 min incubation at room temperature in the dark, an additional 400 μL of 1 × binding buffer was added. Samples were analyzed within 1 h after the staining procedure. Sample analysis was also performed using an EPICS XL flow cytometer.

Antibodies

The following antibodies were used for Western blotting; anti-P53 (BP53-12, diluted 1:500; Novocastra Lab., Claremont Place, United Kingdom), anti-Bax (P-19, 1:250; Santa Cruz Biotechnology, Santa Cruz, CA), anti-Bcl-2 (100, 1:250; Santa Cruz Biotechnology, Santa Cruz, CA), anti-caspase-3 (CCP32, 1:250; Transduction Laboratories, Lexington, KY) and anti-β-actin (Ab-1,1:1500; SIGMA, St. Louis, MO).

Expression of apoptosis related protein

Both floating and attached cells were harvested from wells at 0, 12, 24, 48 and 72 h incubation times after HSV-tk/GCV treatment, and solubilized in lysis buffer with 50 mM Tris-HCl (pH 7.4), 125 mM NaCl, 0.1% NP-40, 1 mM phenyl methyl sulfonyl fluoride, 1 ng/mL leupeptin, 10 ng/mL soy bean trypsin inhibitor, 1 ng/mL aprotinin, 10 ng/mL *N*-tosyl-L-phenylalanyl chloromethyl ketone for 1 h on ice. Lysates were centrifuged at 15,000 rpm for 10 min and then supernatants were decanted. Protein concentrations were determined using the Bradford protein assay (Bio-Rad Lab., Richmond, CA). Equal amounts (25 μg) of total protein were loaded onto each lane of 10% SDS polyacrylamide gels, electrotransferred to a polyvinylidene difluoride membrane (Millipore, Bedford, MA), and then probed with the respective antibodies. Blots were developed with peroxidase-labeled anti-mouse or anti-rabbit antibodies (1:2000; MBL, Nagoya, Japan) using enhanced chemiluminescence (ECL detection system; Amersham, Bucks, United Kingdom).

TUNEL method

Cells cultured on cover slips were transduced and incubated for 24, 48 and 72 h with and without GCV (1 μg/mL). After incubation, attached cells were washed with PBS twice. Terminal deoxynucleotidyl transferase-mediated dUTP-digoxigenin nick-end labeling (TUNEL) staining was performed according to kit protocol with minor modification using an Apop Tag Plus peroxidase In Situ Apoptosis Detection Kit (Intergen, Purchase, NY). Briefly, after fixation with 95% ethanol, cells were exposed to terminal deoxynucleotidyl transferase with digoxigenin-11-dUTP and dATP in a moist chamber for 90 min at 37˚C. Antidigoxigenin antibody-peroxidase was used for detection of digoxigenin-11-dUTP labeling for 30 min at room temperature, followed by color development with 3,3'-diaminobenzidine containing H_2O_2 solution. Methyl green was used for counterstaining.

Morphological examinations

Both floating and attached cells were harvested from wells at 72 h with and without GCV (1 μg/mL) in all cell lines. After centrifugation and washing with PBS twice, cell pellets were fixed in Kalnovsky solution for 4 h at 4˚C. After overnight

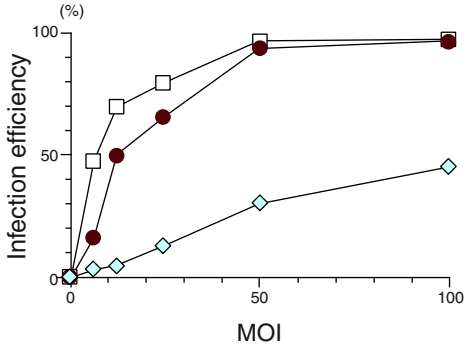

Fig. 1. Adenovirus infection efficiency in oral SCC cell lines. Cells were infected with Ad.β-gal at varying MOIs of 0, 6.25, 12.5, 25, 50 or 100 pfu/cell, respectively. At 48 h after the infection, cells were fixed and stained by X-gal. The percentages of cells expressing the transgene were counted. Infection efficiency was expressed by the percent average of blue-staining cells in three randomly selected × 200 microscopic fields. □, HSC-3, ◇, HSC-4 and ●, SCCKN.

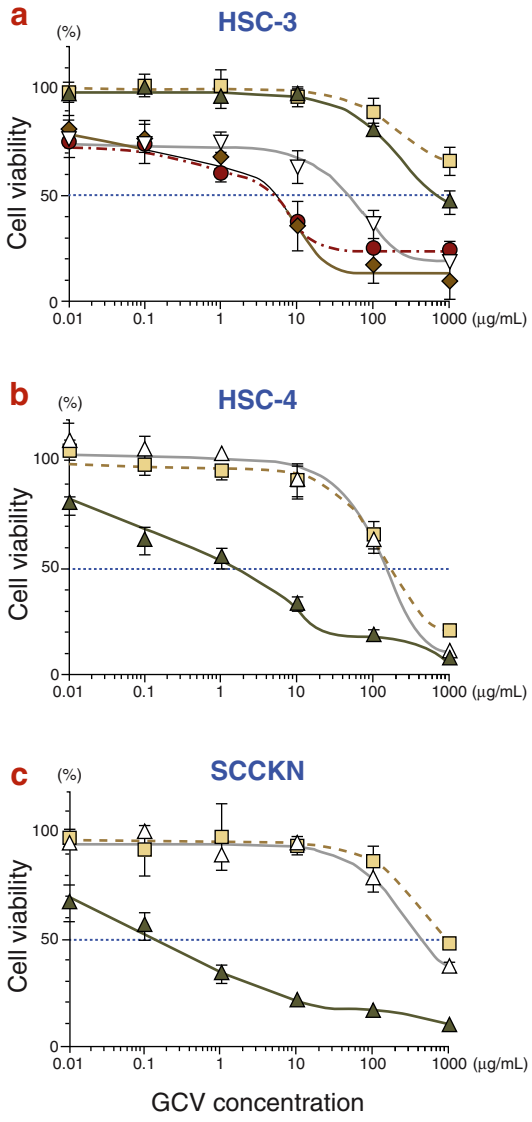

Fig. 2. Cell viabilities after HSV-tk/GCV treatment. Infected cells with either Ad.tk or Ad.β-gal were treated with GCV at concentrations ranging from 0 to 1,000 μg/mL. Uninfected cells without GCV treatment were used as control. Cell viabilities were measured at 96 h after GCV treatment using the MTT assay. Results were calculated as the percentage of viability relative to control. The result represents the mean ± SE of triplicates. The IC_{50} were determined. (**a**) HSC-3, (**b**) HSC-4 and (**c**) SCCKN cell lines. □, GCV alone; △, Ad.β-gal + GCV; ▲, Ad.tk 1.25 MOI + GCV; ▽, Ad.tk5 MOI + GCV; ◆, Ad.tk 10 MOI + GCV and ●, Ad.tk 20 MOI + GCV.

washing with 0.1 M phosphate solution buffered at pH 7.4 at 4˚C, cell pellets were postfixed in 1% osmium tetroxide solution for 2 h. After washing with 0.1 M phosphate solution buffered at pH 7.4, cell pellets were dehydrated in a graded ethanol series and embedded in Epon 812. After polymerization, 1 μm semi-thin sections were served for light microscopic examinations after toluidine blue staning. Then 60 nm ultra-thin sections were served for electron microscopic examination after uranyl acetate and Reynold's lead citrate staining. Specimens were examined with an H-800 electron microscope (Hitachi, Tokyo).

Results

Adenovirus infection efficiency

Adenovirus infecction efficiencies in human oral SCC cell lines were quantified using direct cell counting with X-gal staining. We assessed the infection efficiency at the 48 h time point, when the β-gal expression level was sufficient. For 100% infection, an MOI 50 was needed for HSC-3 and SCCKN cell lines, and impossible for the HSC-4 cell line within an MOI 100 (Fig. 1). However, infection of Ad.tk at these high titers failed to be cytotoxic to oral SCC cell lines. Then we performed an MOI escalation study to determine the sublethal

MOI value of Ad.tk infection (data not shown). The results showed MOIs of 20 and less for the HSC-3 cell line and 2.5 and less for HSC-4 and SCCKN cell lines, respectively.

Cell viability

Cell viability was determined from the colorimetric quantity of viable cells. HSV-tk gene transfer decreased the median inhibitory concentration (IC_{50}) at least 2 logs lower in all cell lines (Fig. 2). Cell viability was dependent on GCV concentration. As the HSC-3 cell line only had resistance to Ad-tk infection, we could examine cell viabilities at several ranges of MOI (Fig. 2a). Though the IC_{50} decreased in proportion to the MOI escalation, the results were not different between MOIs of 20 and 10. This fact suggested the upper limit bounds of MOI escalation of this strategy.

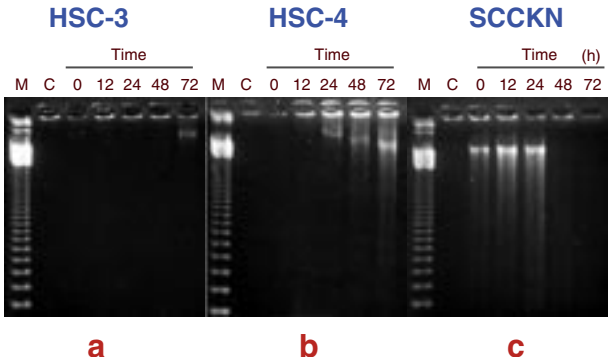

Fig. 3. DNA fragmentation after HSV-tk/GCV treatment. Cells were infected with Ad.tk at MOI 5 for HSC-3, 2.5 for HSC-4 and SCCKN, and followed by 1 μg/mL GCV. Cells were harvested in a time-dependent manner. Uninfected cells without GCV treatment were used as control. DNA extracts were loaded on 2% agarose gel by electrophoresis and visualized by staining with 0.5 μg/mL ethidium bromide. (**a**) HSC-3, (**b**) HSC-4 and (**c**) SCCKN cell lines. M, marker; C, control.

DNA fragmentation

Internucleosomal DNA fragmentation was examined for standard apoptotic hallmarks. They all showed smearing, whose peaks were 72 h, 72 h and 24 h for cell lines HSC-3, HSC-4 and SCCKN, respectively (Fig. 3).

Cell cycle kinetics

Figure 4 shows the results of cell cycle kinetic analysis. The cells broke down severely showing a time-dependent decrease of G1 and G2/M peaks without cell cycle arrest. Sub-G1 fraction, which means hypodiploid cells correspond to dead cells,

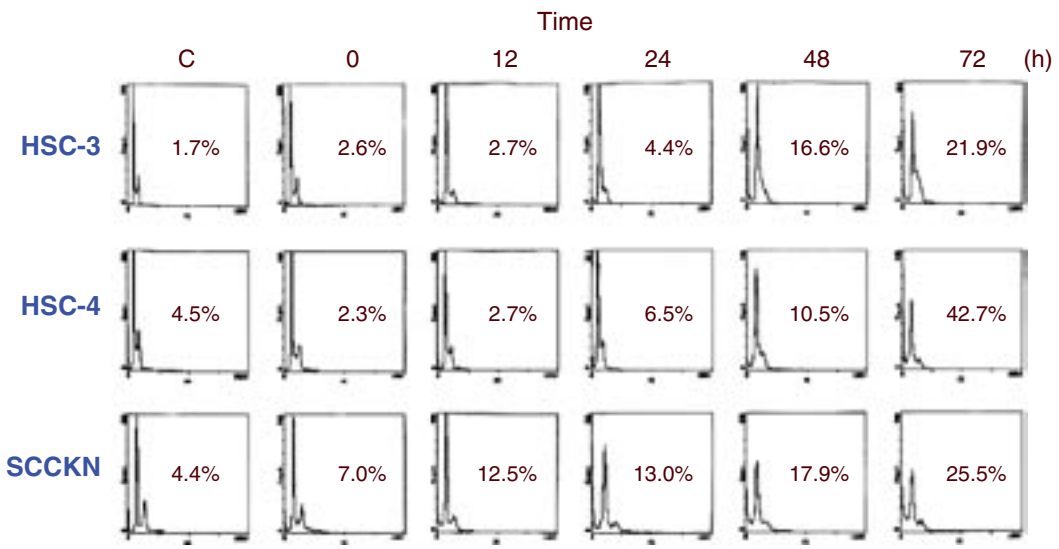

Fig. 4. Cell cycle kinetics analysis by flow cytometry. Cells were infected with Ad.tk at MOI 5 for HSC-3, 2.5 for HSC-4 and SCCKN, and followed by 1 μg/mL GCV. Cells were harvested in a time-dependent manner. Uninfected cells without GCV treatment were used as control. The number within each panel shows the percentage of Sub-G1 fractions. C, control.

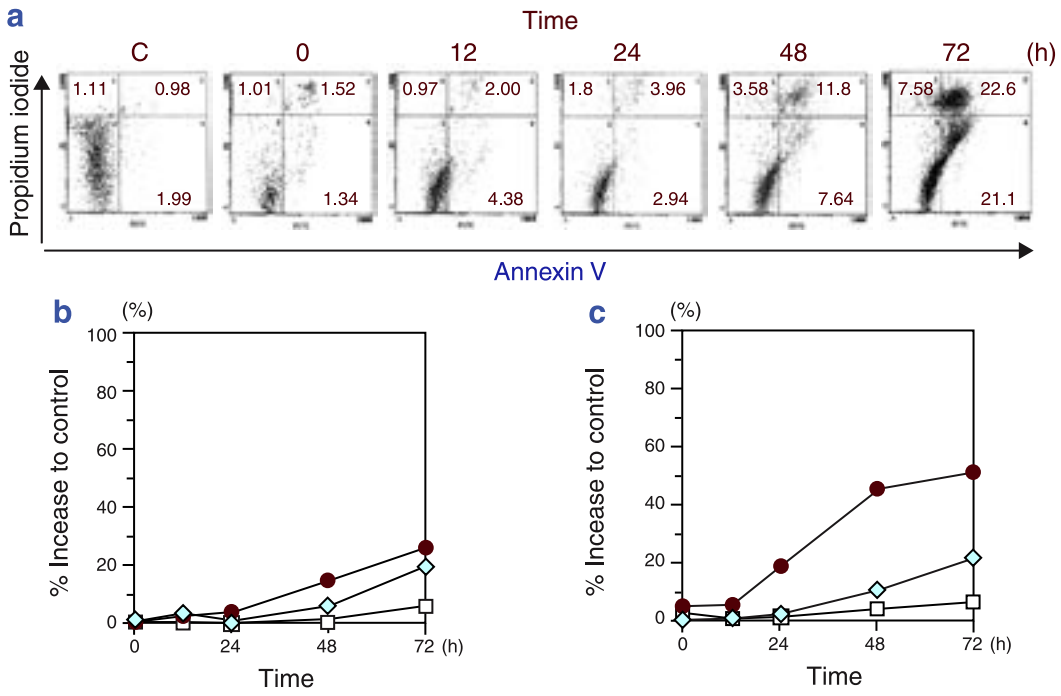

Fig. 5. Annexin V-FITC and PI double stainning by flow cytometry. Cells were infected with Ad.tk at MOI 5 for HSC-3, 2.5 for HSC-4 and SCCKN, and followed by 1 μg/mL GCV. Cells were harvested in a time-dependent manner. Uninfected cells without GCV treatment were used as control.

a: Representative results of HSC-4. The number within each panel shows the percentage of each quadrant. C, control.

b: Increases in percentage in the lower right quadrant relative to control. □, HSC-3, ◇, HSC-4 and ●, SCCKN.

c: Increases in percentage in the upper right quadrant relative to control. □, HSC-3, ◇, HSC-4 and ●, SCCKN.

increased in a time-dependent manner in all the cell lines.

Annexin V assay

Annexin V has an affinity for the phosphatidylserine that is translocated from the inner leaflet to the outer leaflet of the plasma membrane in the early stage of apoptosis (Martin et al., 1995). During the late stage, the plasma membrane showed increased permeability and PI entered the cytoplasm and stained chromatin indicating necrosis. Figure 5a shows representative kinetics of HSC-4 in the cell lines. The proportion of annexin V-positive/PI-negative cells in the lower right quadrant shows the early stage of apoptosis increased in a time-dependent manner (Fig. 5b). The proportion of annexin V-positive/PI-positive in the upper right quadrant shows necrosis also increased in a time-dependent manner (Fig. 5c).

Expression of apoptosis related protein

Protein expression levels of P53, P21, Bax, Bcl-2 and caspase-3 activation were examined by Western blot analysis (Fig. 6). P53 was stably expressed in HSC-3 and HSC-4 cell lines, and undetectable at all time points in the SCCKN cell line. P21 and Bax was consistently expressed at any time points in all cell lines. On the other hand, Bcl-2 slightly but steadily increased within 24 h after treatment in HSC-3 and SCCKN cell lines. No caspase-3 cleavage or activation was observed throughout the experiment in any cell lines.

TUNEL method

In situ DNA strand breaks were examined by the TUNEL method. TUNEL-positive cells with brown-labeled nuclei were occasionally detected

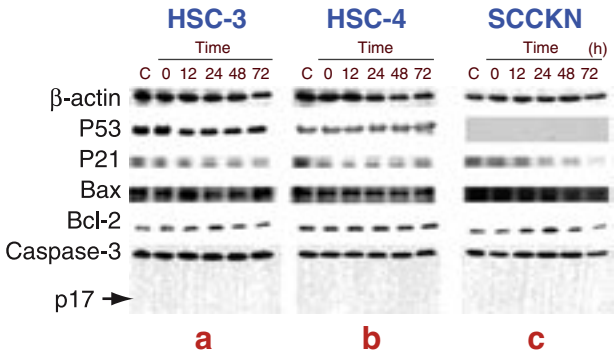

Fig. 6. Western blot analysis of P53, P21, Bax, Bcl-2 and caspase-3 of each cell lines. Cells were infected with Ad.tk at MOI 5 for HSC-3, 2.5 for HSC-4 and SCCKN, and followed by 1 μg/mL GCV. Cells were harvested in a time-dependent manner. Uninfected cells without GCV treatment were used as control. (**a**) HSC-3, (**b**) HSC-4 and (**c**) SCCKN cell lines. C, control.

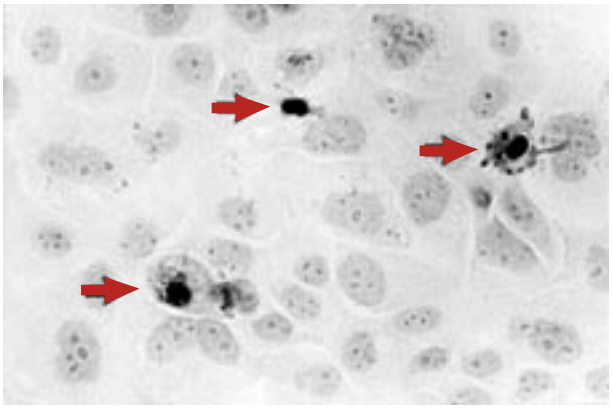

Fig. 7. TUNEL staining of treated SCCKN 24 h after GCV treatment. Cells were infected with Ad.tk at MOI 2.5, and followed by 1 μg/mL GCV. TUNEL-positive cells with brown-labeled nuclei are occasionally detected in only SCCKN cell line (arrows).

in only the SCCKN cell line infected with Ad.tk at MOI 2.5 followed by 1 μg/mL GCV after 24 h (Fig. 7). However, we could not evaluate correctly at 48 h and 72 h because most treated SCCKN cells had easily come off in the staining procedure. However, the untreated SCCKN cells showed no TUNEL signal.

Morphological examinations

There were no significant differences in morphological findings in both semi-thin and ultra-thin sections after HSV-tk/GCV treatment among the cell lines. Semi-thin sections of untreated cells showed variations in size and shape and occasionally small vesicles in the cytoplasm with a few mitoses (Fig. 8a). In contrast, a large number of treated cells became swollen with or without membrane disruption, sometimes involving nuclei disruption (Fig. 8b). Cytoplasmic vesicles were markedly increased. There were few cells with chromatin aggregation in HSC-4 and SCCKN cell lines.

Ultra-thin sections revealed intact nuclei, intracellular organelles and their membranes in untreated cells (Fig. 9a). Otherwise, a large number of treated cells contained enlarged and rounded nuclei in which heterochromatin was sparse. Cytoplasmic membranes were also disrupted (Fig. 9b). A few cells showing chromatin aggregation to the nuclear membranes, also displayed cytoplasmic membranes disruption. Treated cells presented structural changes of intracellular organelles involving enlargement of mitochondria with the disappearance of cristae, vesiculation and vacuolization of endoplasmic reticulum. Apoptotic bodies were not observed in any of the treated cells.

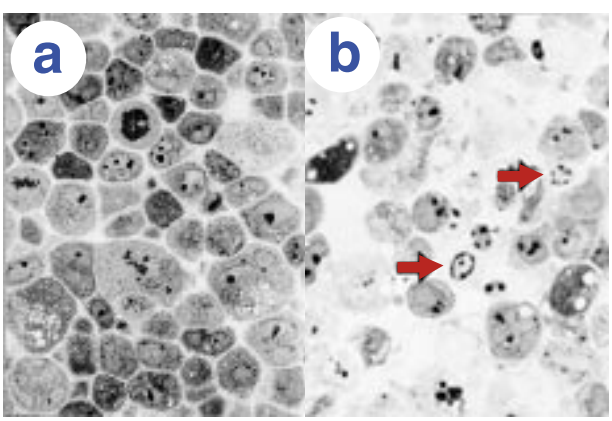

Fig. 8. Semi-thin section micrographs of HSC-4 cells. (**a**) Untreated cells. Some cells occasionally have small vesicles, and some display mitoses. (**b**) Treated cells 72 h after GCV treatment. Cells were infected with Ad.tk at MOI 2.5, and followed by 1 μg/mL GCV. Cells become swollen and intracytoplasmic vesicles remarkably increase. Few cells show chromatin aggregation (arrows).

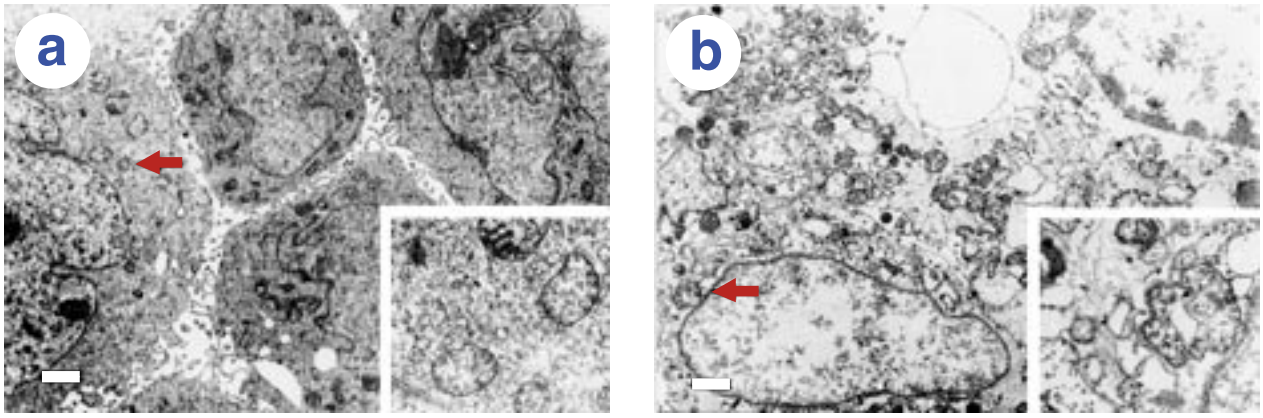

Fig. 9. Ultra-thin section micrograph of HSC-4 cells. (**a**) Untreated cells. (**b**) Treated cells 72 h after GCV treatment. Cells were infected with Ad.tk at MOI 2.5, and followed by 1 μg/mL GCV. A large number of cells contain enlarged and rounded nuclei of which hetero chromatin are sparse. Some of treated cells show chromatin aggregation. But their cytoplasmic membranes are still disruptured. Inset of (**b**) displays enlargement of mitochondria with disappearance of cristae, vesiculation and vacuolization of endoplasmic reticula. Bars in (**a**) and (**b**) = 1 μm.

Discussion

This study clearly demonstrated that HSV-tk/GCV treatment showed diverse but obvious sensitivity to oral SCC cell lines independent of their histological status (Table 1 and Fig. 2). Oral SCC cell lines displayed high susceptibility to HSV-tk/GCV treatment despite low transduction, suggesting possible tumoricidal effects even in the case of inability of 100% gene delivery (Fig. 1). In the HSC-3 cell line, however, HSV-tk/GCV treatment showed the upper limit bounds at MOI 10. As reported previously, a higher expression of HSV-tk gene may not be able to further enhance the tumoricidal effect, though a threshold level of HSV-tk gene expression is necessary for maximum cell killing (Chen et al., 1995).

The tumoricidal mechanism of HSV-tk/GCV treatment has focused on exploring the molecular biological events associated with apoptosis (Samejima and Maruelo, 1995; Wei et al., 1998; Rivas et al., 2001). To date, the most reliable method for identifying apoptotic cell death is the detection of the occurrence of internucleosomal DNA strand breaks (Wyllie, 1980). Concerning past HSV-tk/GCV treatment studies, several reported the existence of DNA laddering (Samejima and Maruelo, 1995; Wei et al., 1998), but several reported the opposite (Kaneko and Tsukamoto, 1995). It is possible that the DNA fragmentation assay might not detect low levels of apoptosis. Confirmation of the phenotype of dying cells is needed by reference to morphology using electron microscopy (Vile et al., 1997). In fact, some cases failed to demonstrate DNA laddering even when the presence of apoptotic cells was further confirmed using electron microscopy (Freeman et al., 1993; Craperi et al., 1999). In the present results, DNA fragmentation showed unspecific DNA degradation, that is, smearing (Fig. 3). Accordingly, both semi- and ultra-thin examinations revealed the phenotype of dying cells was necrotic in all cell lines.

Previous studies of flow cytometry demonstrated that HSV-tk/GCV treatment caused either S- and/or G2/M-phase cell cycle arrest before undergoing cell death (Kaneko et al., 1995; Wei et al., 1998; Craperi et al., 1999). The present results showed cell death progressing with no cell cycle arrest (Fig. 4). The DNA content of sub-G1 increased in a time-dependent manner. A rapid increase was observed in the HSC-4 cell line at 72 h (42.7%), in which DNA fragmentation definitely showed smearing suggesting no occurrence of regular DNA double-strand breaks. Annexin V has been used as another biological marker to detect the early stage of apoptosis before the occurrence

of morphological changes in single cells (Martin et al., 1995). The present results showed that annexin V-positive/PI-negative cells corresponding to apoptotic cells, increased in a time-dependent manner in all cell lines (Fig. 5b), although further semi- and ultra-thin examinations revealed necrotic morphological features. While the externalization of phosphatidylserine during apoptosis has been presented, intracellular events have not been adequately elucidated. Although the meaning of the annexin V-positive reaction induced by HSV-tk/GCV treatment is not contested, this phenomenon implies the feasibility of inspection and exemplification by phagocytic cells (Depraetere, 2000; Hanayama et al., 2002). Changes in the properties of their surface membrane would improve the combination with a targeting approach such as immunotherapy.

Since the tumoricidal effect of HSV-tk/GCV treatment is conceivable via DNA damage, the loss of function of p53 can develop resistance to apoptosis. Li et al. reported, however, the HSV-tk/GCV cytotoxic response did not depend on the expression of a functional p53 (Li et al., 1999; Craperi et al., 1999). Similarly, we demonstrated an obvious tumoricidal effect without either p53 or p21 expression (Figs. 4 and 6). These results were consistent in all cell lines and suggested that p53-dependent cell cycle regulation or apoptosis induction may not correlate with the tumoricidal effect of HSV-tk/GCV treatment to oral SCC. Alternatively, HSV-tk/GCV treatment might have considerable potential to oral SCC that highly expresses mutated p53 *in vivo* (Naglar et al., 2002) and *in vitro* (Sakai and Tsuchida, 1992). A previous exogenous *p53* transduction study suggested co-expression of p53 did not enhance the cytotoxicity of HSV-tk/GCV treatment, although p53 was able to increase amount of apoptosis which was markedly less than the total cell death *in vitro* (Xie et al., 1999).

Dimerization between Bax and Bcl-2 is an important factor to direct either death promotion or death inhibition. Bax accumulation was reported after GCV exposure in glioma cell lines (Craperi et al., 1999). However, they could not rule out the possible occurrence of necrotic cell death. In contrast, over-expression of Bcl-2 inhibited HSV-tk/GCV-induced activation of caspase and apoptosis (Beltinger et al., 2000). However, no synchronous correlation could be found between the expression levels of Bcl-2 family and the sensitivity to the oral SCC cell lines.

No cleavage or activation of caspase-3 was detected in oral SCC cell lines. This suggested the existence of an alternative molecular pathway responsible for the tumoricidal effect of HSV-tk/GCV treatment to oral SCC cell lines even though the route of cell death is unknown.

One exception in the present study was an occasional positive TUNEL signal in SCCKN cells (Fig. 7). However, no other evidence of apoptosis was detected with other biological assays. Cautionary notes suggested that a positive TUNEL signal should not be considered as a specific marker of apoptosis because the assay would also suggest necrotic cell death (Charriaut-Marlangue and Ben-Ari, 1995; Grask-kraupp et al., 1995).

Apoptosis was originally described on the basis of the morphological features by electron microscopy (Kerr et al., 1972) even though some features may also be detectable by light microscopy. Apoptotic bodies including cellular remnants should be observed either in the intercellular space or within the cytoplasm of intact cells. A large number of treated cells showed disintegration of the cell structure involving irregular scattered heterochromatin, swelling of cytoplasm and intracellular organelles, and cytoplasmic membrane disruption in all cell lines. Furthermore, intact cells containing apoptotic bodies that deposit the fragmented components from neighboring dead cells were not found. Based on the annexin V/PI double staining at 72 h, the HSC-4 cell line should include the cells of early stage apoptosis of 19.1% (Fig. 5). However, we could not find firm evidence of apoptosis in semi- and ultra-thin section examinations. Consequently, apoptosis may not play a central role in the tumoricidal mechanism. The hypothesis that the bystander effect is mediated by phagocytosis is unacceptable for oral SCC cells *in vitro*.

A previous study using Fas ligand demonstrated an artificial deficiency of caspase-8 resulted

in a switch of cell death from apoptosis to necrosis in Jurket cell lines (Kawahara et al., 1998). This implies that caspase activation itself was dispensable for determining cell death. Kitanaka and Kuchino (1999) suggested the existence of caspase-independent programmed cell death with necrotic-like morphology, that can be activated either alone or in concert with the caspase-dependent apoptotic program. Differential sensitivity and the type of cell death induced by HSV-tk/GCV treatment appear to be dependent upon cell-type difference, in addition to the status of the apoptosis-related gene.

In summary, we demonstrated that oral SCC cell lines exhibited an obvious sensitivity to HSV-tk/GCV treatment suggesting the presence of a p53- and caspase-3-independent death signaling pathway. However, the mechanism and the molecular pathway responsible for HSV-tk/GCV-induced cell death are still unknown. A better understanding of the cell death mechanism is essential to establish an appropriate and effective modality in future studies.

Acknowledgments: All authors thank Professor Kenzo Sato (Division of Molecular Biology, Department of Molecular and Cellular Biology, School of Medicine, Tottori University Faculty of Medicine) for his appropriate advice and kindly providing two replication-deficient recombinant adenovirus vectors, Ad.β-gal and Ad.tk. We also thank Professor Kazuo Yamada (Division of Medical Biochemistry, Department of Pathophysiological and Therapeutic Science, School of Medicine, Tottori University Faculty of Medicine) for his invaluable advice, and Mr. Norihisa Itaki (Division of Organ Pathology, Department of Microbiology and Pathology, School of Medicine, Tottori University Faculty of Medicine) for his skilful technical assistance. Finally, we thank all the members of Division of Organ Pathology, Department of Microbiology and Pathology, School of Medicine, Tottori University Faculty of Medicine for their helpful discussions.

References

1 Beltinger C, Fulda S, Kammertoens T, Meyer E, Uckert W, Debatin KM. Herpes simplex virus thymidine kinase/ganciclovir-induced apoptosis involves ligand-independent death receptor aggregation and activation of caspases. Proc Natl Acad Sci U S A 1999;96:8699–8704.

2 Beltinger C, Fulda S, Kammertoens T, Uckert W, Debatin KM. Mitochondrial amplification of death signals determines thymidine kinase/ganciclovir-triggered activation of apoptosis. Cancer Res 2000; 60:3212–3217.

3 Bi WL, Parysek LM, Warnick R, Stambrook PJ. In vitro evidence that metabolic cooperation is responsible for the bystander effect observed with HSV tk retroviral gene therapy. Hum Gene Ther 1993;4: 725–731.

4 Borrelli E, Heyman R, Hsi M, Evans RM. Targeting of an inducible toxic phenotype in animal cells. Proc Natl Acad Sci U S A 1988;85:7572–7576.

5 Boucher PD, Ruch RJ, Shewach DS. Differential ganciclovir-mediated cytotoxicity and bystander killing in human colon carcinoma cell lines expressing herpes simplex virus thymidine kinase. Hum Gene Ther 1998;9:801–814.

6 Charriaut-Marlangue C, Ben-Ari Y. A cautionary note on the use of the TUNEL stain to determine apoptosis. Neuroreport 1995;7:61–64.

7 Chen CY, Chang YN, Ryan P, Linscott M, McGarrity GJ, Chiang YL. Effect of herpes simplex virus thymidine kinase expression levels on ganciclovir-mediated cytotoxicity and the "bystander effect". Hum Gene Ther 1995;6:1467–1476.

8 Colombo BM, Benedetti S, Ottolenghi S, Mora M, Pollo B, Poli G, et al. The "bystander effect": association of U-87 cell death with ganciclovir-mediated apoptosis of nearby cells and lack of effect in athymic mice. Hum Gene Ther 1995;6:763–772.

9 Craperi D, Vicat JM, Nissou MF, Mathieu J, Baudier J, Benabid AL, et al. Increased bax expression is associated with cell death induced by ganciclovir in a herpes thymidine kinase gene-expressing glioma cell line. Hum Gene Ther 1999;10:679–688.

10 Depraetere V. "Eat me" signals of apoptotic bodies. Nat Cell Biol 2000;2:E104.

11 Elion GB. Mechanism of action and selectivity of acyclovir. Am J Med 1982;73:7–13.

12 Freeman SM, Abboud CN, Whartenby KA, Packman CH, Koeplin DS, Moolten FL, et al. The "bystander effect": tumor regression when a fraction of the tumor mass is genetically modified. Cancer Res 1993;53:5274–5283.

13 Fukui T, Hayashi Y, Kagami H, Yamamoto N, Fukuhara H, Tohnai I, et al. Suicide gene therapy for human oral squamous cell carcinoma cell lines with adeno-associated virus vector. Oral Oncol 2001;37:211–215.

14 Glaser T, Castro MG, Lowenstein PR, Weller M. Death receptor-independent cytochrome c release

and caspase activation mediate thymidine kinase plus ganciclovir-mediated cytotoxicity in LN-18 and LN-229 human malignant glioma cells. Gene Ther 2001;8:469–476.
15 Grasl-Kraupp B, Ruttkay-Nedecky B, Koudelka H, Bukowska K, Bursch W, Schulte-Hermann R. In situ detection of fragmented DNA (TUNEL assay) fails to discriminate among apoptosis, necrosis, and autolytic cell death: a cautionary note. Hepatology 1995;21:1465–1468.
16 Hanayama R, Tanaka M, Miwa K, Shinohara A, Iwamatsu A, Nagata S. Identification of a factor that links apoptotic cells to phagocytes. Nature 2002;417:182–187.
17 Kaneko Y, Tsukamoto A. Gene therapy of hepatoma: bystander effects and non-apoptotic cell death induced by thymidine kinase and ganciclovir. Cancer Lett 1995;96:105–110.
18 Katabi M, Yuan S, Chan H, Galipeau J, Batist G. The nonapoptotic pathway mediating thymidine kinase/ganciclovir toxicity is reduced by signal from adenovirus type 5 early region 4. Mol Ther 2002;5: 170–176.
19 Kawahara A, Ohsawa Y, Matsumura H, Uchiyama Y, Nagata S. Caspase-independent cell killing by Fas-associated protein with death domain. J Cell Biol 1998;143:1353–1360.
20 Kerr JF, Wyllie AH, Currie AR. Apoptosis: a basic biological phenomenon with wide-ranging implications in tissue kinetics. Br J Cancer 1972;26:239–257.
21 Kitanaka C, Kuchino Y. Caspase-independent programmed cell death with necrotic morphology. Cell Death Differ 1999;6:508–515.
22 Lanuti M, Gao GP, Force SD, Chang MY, El Kouri C, Amin KM, et al. Evaluation of an E1E4-deleted adenovirus expressing the herpes simplex thymidine kinase suicide gene in cancer gene therapy. Hum Gene Ther 1999;10:463–475.
23 Li PX, Ngo D, Brade AM, Klamut HJ. Differential chemosensitivity of breast cancer cells to ganciclovir treatment following adenovirus-mediated herpes simplex virus thymidine kinase gene transfer. Cancer Gene Ther 1999;6:179–190.
24 Martin SJ, Reutelingsperger CP, McGahon AJ, Rader JA, van Schie RC, LaFace DM, et al. Early redistribution of plasma membrane phosphatidylserine is a general feature of apoptosis regardless of the initiating stimulus: inhibition by overexpression of Bcl-2 and Abl Iodine-124 labelled Annexin-V as a potential radiotracer to study apoptosis using positron emission tomography. J Exp Med 1995;182: 1545–1556.
25 Moolten FL, Wells JM, Heyman RA, Evans RM. Lymphoma regression induced by ganciclovir in mice bearing a herpes thymidine kinase transgene. Hum Gene Ther 1990;1:125–134.
26 Nagler RM, Kerner H, Laufer D, Ben-Eliezer S, Minkov I, Ben-Itzhak O. Squamous cell carcinoma of the tongue: the prevalence and prognostic roles of p53, Bcl-2, c-erbB-2 and apoptotic rate as related to clinical and pathological characteristics in a retrospective study. Cancer Lett 2002;186:137–150.
27 O'Malley BW, Cope KA, Chen SH, Li D, Schwarta MR, Woo SL. Combination gene therapy for oral cancer in a murine model. Cancer Res 1996;56: 1737–1741.
28 Rivas C, Miller AR, Collado M, Lam EW, Apperley JF, Melo JV. BCR-ABL-expressing cells transduced with the HSV-tk gene die by apoptosis upon treatment with ganciclovir. Mol Ther 2001;3:642–652.
29 Sakai E, Tsuchida N. Most human squamous cell carcinomas in the oral cavity contain mutated p53 tumor-suppressor genes. Oncogene 1992;7:927–933.
30 Samejima Y, Meruelo D. "Bystander killing" induces apoptosis and is inhibited by forskolin. Gene Ther 1995;2:50–58.
31 Vile RG, Castleden S, Marshall J, Camplejohn R, Upton C, Chong H. Generation of an anti-tumour immune response in a non-immunogenic tumour: HSVtk killing in vivo stimulates a mononuclear cell infiltrate and a Th1-like profile of intratumoural cytokine expression. Int J Cancer 1997;71:267–274.
32. Wei SJ, Chao Y, Hung YM, Lin WC, Yang DM, Shih YL, et al. S- and G2-phase cell cycle arrests and apoptosis induced by ganciclovir in murine melanoma cells transduced with herpes simplex virus thymidine kinase. Exp Cell Res 1998;241:66–75.
33 Wyllie AH. Glucocorticoid-induced thymocyte apoptosis is associated with endogenous endonuclease activation. Nature 1980;284:555–556.
34 Xie Y, Gilbert JD, Kim JH, Freytag SO. Efficacy of adenovirus-mediated CD/5-FC and HSV-1 thymidine kinase/ganciclovir suicide gene therapies concomitant with p53 gene therapy. Clin Cancer Res 1999;5:4224–4232.

Received June 20, 2005; accepted August 29, 2005

Corresponding author: Mitsuhiko Osaki, PhD